

Article

Optimizing Curdlan Synthesis: Engineering *Agrobacterium tumefaciens* ATCC31749 for Enhanced Production Using Dextrin as a Carbon Source

Tingting Yu ^{1,2} , Yu Wang ^{1,2}, Wei Wang ^{1,2}, Yonggang Zhang ^{1,2}, Yanmin Zhang ^{1,2}, Hongyu Han ^{1,2}, Yang Liu ^{1,2}, Siduo Zhou ^{1,2} and Xueqian Dong ^{1,2,*} 

¹ Faculty of Food Science and Engineering, Qilu University of Technology (Shandong Academy of Sciences), Jinan 250353, China; 17861408785@163.com (T.Y.); wangwei87@qlu.edu.cn (W.W.)

² Shandong Research and Design Institute of Food & Fermentation Industry, Jinan 250013, China

* Correspondence: dxq@qlu.edu.cn

Abstract: A key goal in current research on industrial curdlan production is the expansion of carbon sources for fermentation. In this study, a recombinant bacterial strain, sp-AmyAXCC, capable of fermenting and synthesizing curdlan using dextrin as a carbon source, was produced via heterologous expression of IPTG-inducible α -amylase from *Xanthomonas campestris* NRRL B-1459 in *Agrobacterium tumefaciens* ATCC31749. External expression of the enzyme was confirmed by western blotting, and the expression levels of exogenous proteins during the fermentation process were monitored. Additionally, the properties of the curdlan product were characterized using attenuated total reflectance-Fourier transform infrared spectroscopy and X-ray diffraction. The recombinant strain produced curdlan at a titer of 30.40 ± 0.14 g/L, gel strength of 703.5 ± 34.2 g/cm², and a molecular weight of 3.58×10^6 Da, which is 33% greater than the molecular weight of native curdlan (2.69×10^6 Da). In the batch fermentation of sp-AmyAXCC with 12% dextrin as a carbon source, the titer of curdlan was 66.7 g/L with a yield of 0.56 g/g, and a productivity rate of 0.62 g/L/h at 108 h. The results of this study expand the substrate spectrum for *Agrobacterium* fermentation in curdlan production and provides guidance for further industrialization of curdlan production.

Keywords: curdlan; *Agrobacterium*; α -amylase; carbon source; genetic engineering



Citation: Yu, T.; Wang, Y.; Wang, W.; Zhang, Y.; Zhang, Y.; Han, H.; Liu, Y.; Zhou, S.; Dong, X. Optimizing Curdlan Synthesis: Engineering *Agrobacterium tumefaciens* ATCC31749 for Enhanced Production Using Dextrin as a Carbon Source. *Fermentation* **2024**, *10*, 240. <https://doi.org/10.3390/fermentation10050240>

Academic Editor: Michael Breitenbach

Received: 19 March 2024

Revised: 26 April 2024

Accepted: 27 April 2024

Published: 30 April 2024



Copyright: © 2024 by the authors. Licensee MDPI, Basel, Switzerland. This article is an open access article distributed under the terms and conditions of the Creative Commons Attribution (CC BY) license (<https://creativecommons.org/licenses/by/4.0/>).

1. Introduction

Curdlan, $(C_6H_{10}O_5)_n$, is an extracellular, non-branched β -1,3-glucan produced through microbial fermentation under nitrogen-limited conditions. Typically, each curdlan molecule consists of 300–500 glucose residues [1] (Figure 1). Aqueous curdlan solutions can form either low-intensity heat-reversible or high-intensity heat-irreversible gels with different structures and properties at different temperatures [2]. Curdlan was first discovered and reported by Tokuya et al. [3] in 1966 and was approved by the U.S. Food and Drug Administration (FDA) in 1996 for use as a food additive. In recent years, the applications of curdlan have expanded continuously; it is now widely used in food processing, aquaculture, oil recovery, biopharmaceuticals, daily chemicals, and other fields. In particular, curdlan is an irreplaceable, high-quality raw material used in the high-end food manufacturing industry [4,5]. Curdlan and its derivatives also exhibit physiological functions, such as antibacterial [6], antitumor [7], antiviral [8], and immune-enhancing [9] activity. Chemical modifications of curdlan, such as sulfation [10], carboxymethylation [11], cationization [12], amination [13], phosphorylation [14], click chemistry [15], oxidation, and esterification [16], can be employed to prepare water-soluble and biologically active curdlan derivatives applicable in the field of biomedicine.

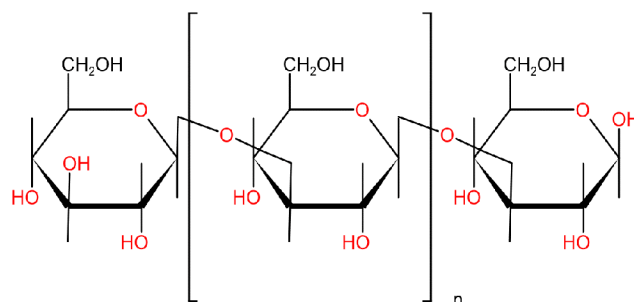


Figure 1. Molecular structure of curdlan.

Microbes capable of curdlan synthesis include *Agrobacterium* sp. [17], *Rhizobium* spp. [18], *Escherichia coli* [19], and *Bacillus subtilis* [20]. Among these, *Agrobacterium* spp. have been widely used in the industrial production of curdlan [21]. Numerous studies have been conducted to enhance curdlan production, including screening or constructing high-yield strains [22,23], optimizing fermentation control strategies [24,25], and improving separation and extraction technologies [26]. Carbon sources are crucial factors in the fermentation industry. Currently, the primary carbon sources for industrial curdlan production are sucrose and glucose. However, sucrose is relatively expensive, and high concentrations of glucose severely inhibit bacterial growth. Therefore, one of the current research hotspots in industrial curdlan production is the expansion of the carbon sources for fermentation. An example of this research is the work of Wan et al. [27], who demonstrated the feasibility of *Agrobacterium* sp. to utilize cassava starch as a substrate for curdlan biosynthesis by supplementing exogenous β -amylase and pullulanase during fermentation. Genetic engineering of curdlan-producing strains has become an efficient means of promoting industrial production. As an example, Shin et al. [28] constructed an *Agrobacterium* sp. strain with a 2.5-fold enhanced capacity to utilize cellobiose to synthesize curdlan by introducing an energy-efficient cellobiose phosphorylase pathway under the control of strong promoters. Gao et al. [29] increased curdlan production by 19% or 17% by deleting the EPS production regulator-encoding gene *exoR* or EPS production repressor protein-encoding gene *exoX*, respectively, in *Agrobacterium* sp. Based on these studies, it is feasible to introduce exogenous enzymes related to substrate utilization into *Agrobacterium* sp. to give the bacteria the ability to use carbon sources other than sucrose and glucose to produce curdlan.

Heterologous expression, which allows for the production of large quantities of specific proteins in different host systems, is a widely used technique that typically involves introducing a target gene (e.g., a DNA sequence encoding a target protein) into a host cell and utilizing the host cell's biological machinery to transcribe and translate the target gene to produce the desired target protein. Heterologous expression has now become a major production method to increase the protein yield of many industrial enzymes such as α -amylase. In order to achieve efficient expression, expression vectors are usually screened and constructed. This mainly includes the selection of suitable expression vectors and strong promoters, etc. PBBR1 plasmids have antibiotic screening markers, small plasmid size (<5.3 kb), and extended multiple cloning sites (MCS) within the *lacZa* gene. They also have the advantage of mobility and compatibility. The strength of promoter activity is the key to realizing the genetic engineering of exogenous expression, and different types of promoters have different mechanisms of action, including constitutive, inducible, and so on.

Starch and dextrin are widely available, low-cost carbon sources that have long been used for the production of another microbial polysaccharide, xanthan gum. The strain *Xanthomonas campestris* can utilize starch to produce xanthan gum because of its highly efficient starch utilization system, which includes amylase, the gene for which has been cloned and expressed in *E. coli*. [30]. The most common curdlan-producing strain, *Agrobacterium* sp. ATCC31749, naturally lacks the relevant enzymes that can utilize starch and dextrin. In this study, a recombinant strain, sp-AmyAXCC, was constructed by introducing the α -amylase from *X. campestris* NRRL B-1459 into *Agrobacterium* sp. ATCC31749, under the control of

2.3. Promoter Screening

Green fluorescent protein (GFP) was used as an indicator for promoter screening. Plasmids pBBR-P_{tac}/P_{tet}/P_{xyI}/P_{Rha}/P_{BAD}-GFP, in which GFP expression was controlled by the corresponding promoter, were transformed into *Agrobacterium* sp. ATCC31749. The transformants were inoculated to 5 mL LB medium with kanamycin and cultured at 30 °C to OD₆₀₀ = 0.6–0.8. The corresponding inducers (IPTG for P_{tac}, AHT for P_{tet}, xylose for P_{xyI}, rhamnose for P_{Rha}, and arabinose for P_{BAD}) were added to the medium, and the cultures were induced overnight. Green fluorescence was observed under blue-light irradiation.

2.4. Plasmid Construction and Transformation

Genomic DNA from *X. campestris* NRRL B-1459 was extracted using a TIANamp Bacteria DNA Kit (Tiangen Biotech Co., Ltd., Beijing, China). Amino acids MRAST-DQETHPMHATSRPCPRTFWQRAHQLLLIALLTTASAQAD of *X. campestris* α -amylase (WP_029217145.1) was predicted to be the signal peptide. To avoid incompatibility of the signal peptide of *X. campestris* α -amylase with the heterologous host, it was substituted with a signal peptide from *Agrobacterium* sp., and the signal peptide of the BMP family ABC transporter substrate-binding protein (WP_262515555.1) was applied. The α -amylase encoding gene was amplified using genomic DNA of *X. campestris* NRRL B-1459 as a template and amy-F1/amy-R1 as primers. The PCR product was used as the template for another round of PCR with amy-F2/amy-R2 as primers to introduce a signal peptide encoding sequence and a 6 × His-tag encoding sequence at its 5' end and 3' end, respectively. Homologous arms for T5 exonuclease-dependent DNA assembly were also included in amy-F2/amy-R2. The pBBR-P_{tac}-GFP plasmid was digested using *Eco*R I and *Nde* I. The second round PCR product and double enzyme digestion product were then used for the construction of recombinant plasmid pBBR-P_{tac}- α -amylase following the One Step SeamlessMix (Ruibo Biotech Co., Ltd., Beijing, China).

The pBBR-P_{tac}- α -amylase plasmid was transformed into *Agrobacterium* sp. by electroporation according to the instructional manual of MicroPulser Electroporator (Bio-Rad, Hercules, CA, USA). Transformants were screened for kanamycin resistance and identified by colony PCR. The correct clone was named sp-AmyAXCC and was stored.

2.5. Expression and Activity Assay of Recombinant α -Amylase

The sp-AmyAXCC was inoculated into LB medium with 50 μ g/mL kanamycin and cultivated at 30 °C. When the OD_{600nm} reached 0.6~0.8, 0.5 mM (final concentration) isopropyl β -D-thiogalactopyranoside (IPTG) was added. After 12 h of induction, the culture was centrifuged, and the supernatant was collected to determine the protein concentration and α -amylase activity. Total protein in the supernatant was extracted via ammonium sulfide precipitation, and the precipitate was resuspended in Tris buffer (50 mM Tris, 200 mM NaCl, pH 8.0). Western blotting with His-tag antibodies was used to confirm the extracellular expression of α -amylase.

A BCA protein assay kit (Tiangen) was used to measure protein concentrations, with bovine serum albumin as the standard. Dextrin is hydrolyzed to glucose by α -amylase, which can be reduced by dinitrosalicylic acid (DNS), and α -amylase activity was analyzed using the DNS assay [31]. To determine the amylase activity, the crude enzyme sample (2 mL) was added to the soluble starch solution (1% *w/v*, 0.5 mL) in phosphate-citrate buffer (50 mM, pH 6.0), DNS was added, and the mixture was incubated at 65 °C for 30 min followed by a boiling water bath for 5 min and cooling in ice water. One amylase unit was taken as the amount of enzyme required to release 1 μ mol of glucose per minute under the given assay conditions.

2.6. Batch Fermentation in Stirred Bioreactors

Batch fermentation was conducted in a 10-L stirred bioreactor (Bailun Biological Technology, Shanghai, China) with 7 L of the initial medium. The fermentation was initiated after inoculation of seed cultures (10% *v/v*) at an OD_{600nm} of 14.95 and carried out

at 30 °C. The initial pH was adjusted to 7.0 and was not controlled during the fermentation process. The aeration rate was 1.0 vvm, and the agitation speed was 300 rpm. IPTG was added to a final concentration of 0.5 mM after 5 h of inoculation. Samples were collected periodically to determine the biomass, α -amylase activity, curdlan yield, and gel strength. Biomass and curdlan yields were determined using the gravimetric method [32]. The sample was centrifuged and 1 mol/L NaOH was added to dissolve the curdlan. After the mixture was centrifuged at $8000 \times g$ for 10 min, the supernatant was collected, the curdlan was precipitated through the addition of 1 mol/L HCl, the pH was adjusted to 7.0, and 95% (v/v) ethanol was added to the supernatant; the mixture was again centrifuged to remove the supernatant, and the precipitate was collected. The precipitate was washed thrice with distilled water, dehydrated with three volumes of ethanol, and freeze-dried. The test was repeated three times for each sample.

2.7. Thermal Gelation Property

Lyophilized curdlan powder was homogenized at 8000 rpm for 10 min, dissolved in deionized water to a final concentration of 20 g/L, and the curdlan solution (10 mL) was transferred into a glass tube (18 mm \times 180 mm). The tube was incubated in a water bath (95 °C) for 10 min and was cooled to ensure the gel formation. A 10 mm long gel section was cut from the bottom of the tube for gel strength measurement using a texture analyzer (Brookfield CT3, Brookfield, WI, USA). The parameters of the compression-mode test were as follows: probe model, TA/35; test speed, 250 mm/min. The gel strength (g) was defined as the maximum force required for gel cracking.

2.8. Molecular Weight Determination of Curdlan

The molecular weight (Mw) of curdlan was measured using an Agilent 1260 Infinity II GPC/SEC (Agilent, Waldbronn, Germany) with double-detector light scattering (LS) and refractive index (RI) [23]. Polymethyl methacrylate (PMMA) was used as a calibration standard to establish this method. The freeze-dried curdlan was completely dissolved in dimethyl sulfoxide (DMSO) with stirring for approximately 4 h at 80 °C. A total of 20 μ L of the curdlan DMSO solution (5.0 mg/mL) was injected into the column (PL Polaegel-M 7.5 \times 50 mm and PL Polaegel-M 7.5 \times 300 mm) by using DMSO as the mobile phase at a flow rate of 1.0 mL/min at 45 °C [33]. The average Mw was calculated using the Agilent 1260 Infinity II GPC/SEC software based on the LS and RI data.

2.9. Fourier-Transform Infrared Spectroscopy and X-ray Diffractometry

The attenuated total reflection Fourier transform infrared (ATR-FTIR) spectra were obtained using a Fourier transform spectrophotometer (Tensor II; Bruker, Karlsruhe, Germany). Curdlan samples were analyzed as described by Wang et al. [34]. In brief, the prepared curdlan solutions were freeze-dried and crushed into a powder, and the samples were assayed using the potassium bromide (KBr) disc method with an average of 64 scans at a resolution of 8 cm^{-1} in the range of 4000–500 cm^{-1} . The XRD pattern of curdlan gum was measured by an XRD diffractometer (Smartlab, Tokyo, Japan). Cu-K α radiation ($\lambda = 0.154$ nm) is produced at 40 kV and 30 mA. XRD analysis was performed at room temperature, at 2θ range of 5° to 80°, a step size of 0.02°, and a scanning speed of 20°/min [35].

3. Results and Discussion

3.1. Promoter Screening

Promoters play important roles in metabolic processes. Using inducible promoters to regulate the expression of recombinant enzymes allows them to be expressed only when needed, thus avoiding the extra metabolic burden on cells as much as possible. To obtain an ideal promoter to regulate the expression of α -amylase, five inducer promoters, P_{BAD} , P_{Rha} , P_{tet} , P_{tac} , and P_{xyl} , were tested in ATCC31749 in this study. Plasmid PBBR- $P_{tac}/P_{tet}/P_{xyl}/P_{Rha}/P_{BAD}$ -GFP, derived from pBBR1MCS-2, was transferred into

ATCC31749, and GFP fluorescence was assayed to evaluate the efficacy and stringency of the promoters. As shown in Figure 2A, only cells harboring GFP regulated by the IPTG-inducible promoter P_{tac} showed a strong difference in fluorescence with or without an inducer, indicating that P_{tac} has both high efficacy and stringency in ATCC31749. As can be seen in Figure 2B,C, the strains in which GFP expression was controlled by P_{BAD} or P_{tet} did not exhibit significant green fluorescence in the presence of the respective inducers (L-arabinose or AHT). This result suggests the low efficiency of these promoters in ATCC31749. In contrast, the strains in which GFP expression was controlled by P_{xyl} or P_{Rha} showed substantial green fluorescence before and after induction with the corresponding inducers (xylose or L-rhamnose) (Figure 2D,E). This indicates high efficiency but poor stringency between the two promoters. Poorly regulated promoters may respond to various conditions or signals, resulting in non-specific gene expression. This can lead to the activation of exogenous genes under undesired conditions, causing unnecessary metabolic processes or protein synthesis. Such nonspecific activation may affect cell growth and metabolic efficiency. Based on these results, P_{tac} was selected to control recombinase expression.

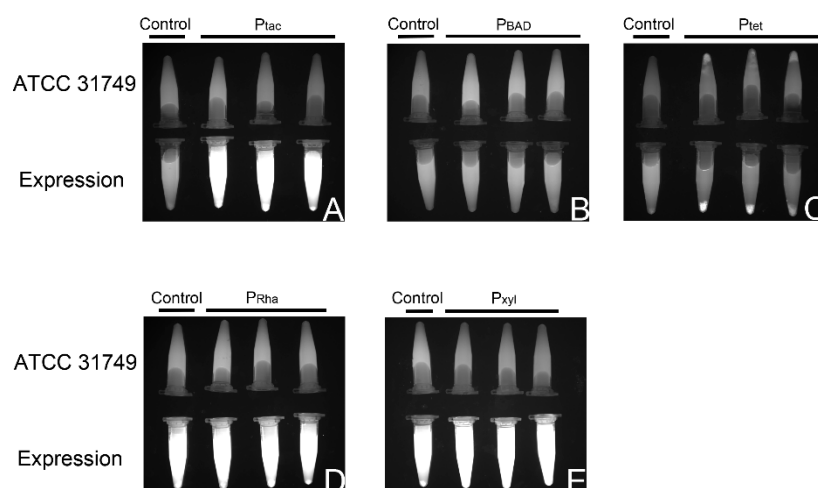


Figure 2. Fluorescence assays of ATCC31749-derived strains in which GFP expressions were regulated by different promoters. (A) GFP expression of ATCC 31749 with pBBR- P_{tac} -GFP. (B) GFP expression of ATCC 31749 with pBBR- P_{BAD} -GFP. (C) GFP expression of ATCC 31749 with pBBR- P_{tet} -GFP. (D) GFP expression of ATCC 31749 with pBBR- P_{Rha} -GFP. (E) GFP expression of ATCC 31749 with pBBR- P_{xyl} -GFP.

3.2. Construction of *sp*-AmyAXCC and Identification of α -Amylase Expression

Agrobacterium sp. are widely used curdolan producers. The strain ATCC31749 is naturally deficient in starch and dextrin utilization. An efficient amylase is required to produce curdolan from dextrin. *X. campestris* is a well-known producer of xanthan gum that efficiently utilizes starch as a substrate. Abe et al. [36] identified an α -amylase that hydrolyzes α -cyclodextrin (α -CD) into maltose and glucose at a high rate in *X. campestris*. Therefore, the *X. campestris* strain NRRL B-1459, which was preserved in our laboratory and exhibits remarkable extracellular amylase activity was chosen to be the supplier of α -amylase. To facilitate the validation of protein expression, a $6 \times$ His-tag was added to the C'-terminus of α -amylase. As shown in Figure 3A, a specific region of the amylase gene was successfully amplified from *X. campestris* NRRL B-1459 genomic DNA. Plasmid pBBR- P_{tac} - α -amylase was constructed by substituting the GFP encoding gene in pBBR- P_{tac} -GFP with the PCR product (Figure 3B) and was then transformed into *Agrobacterium* sp. ATCC31749 to obtain strain *sp*-AmyAXCC (Figure 3C).

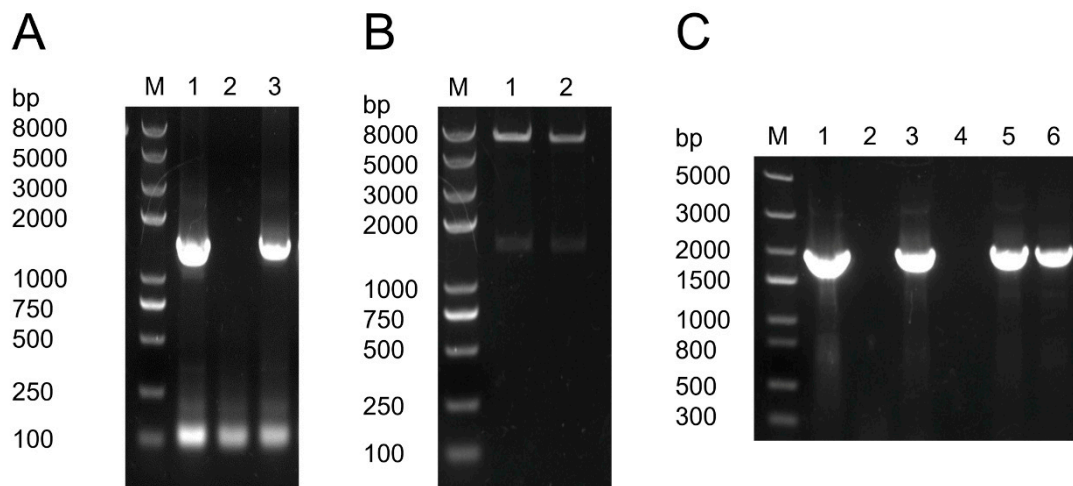


Figure 3. Construction of strain sp-AmyAXCC by introducing α -amylase from *X. campestris* NRRL B-1459 into *Agrobacterium* sp. ATCC31749. (A) PCR amplification of α -amylase encoding gene. Lane M: Trans2K Plus II DNA Marker; lane 1: positive control; lane 2: negative control; lane 3: PCR product with *X. campestris* NRRL B-1459 genomic DNA as the template. (B) Double enzyme digestion of plasmid pBBR-Ptac- α -amylase. Lane M: Trans2K Plus II DNA Marker; lane 1 and lane 2: pBBR-Ptac- α -amylase digested by EcoR I and Nde I. (C) Colony PCR validation of the transformants. Lane M: Trans5K DNA Marker; lane 1: positive control; lane 2: negative control; lane 3–6: PCR products of different colonies.

To validate the extracellular expression of *X. campestris* α -amylase in sp-AmyAXCC, the constructed strain was cultivated and induced with IPTG for 12 h. Western blot analysis using a His-tag specific antibody on the sample of sp-AmyAXCC revealed a single band with an Mw ranging from 40 to 53 kDa, which is absent for wild-type ATCC31749 and corresponds to the target protein (Figure 4). This further confirms the expression of α -amylase in *Agrobacterium* sp. ATCC31749. After 12 h of induction, the amylase activity in the sp-AmyAXCC supernatant was 584.5 U/mL, and the specific enzyme activity was estimated to be 5467 U/mg. These results indicate that the sp-AmyAXCC strain constructed in this study can successfully express active α -amylase extracellularly under IPTG induction.

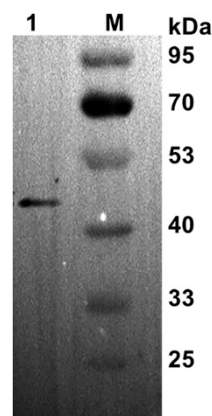


Figure 4. Validation of the extracellular expression of α -amylase by sp-AmyAXCC. Western Blot of the total proteins of ATCC31749 and sp-AmyAXCC culture supernatants. Lane M: Mw Marker; lane 1: ATCC31749 culture supernatant; lane 2: sp-AmyAXCC culture supernatant.

3.3. Curdlan Productions by *sp-AmyAXCC*

Gel strength is a crucial indicator of the gelatin properties of curdlans. Typically, strain ATCC31749 cannot produce curdlan when using starch or dextrin as the substrate, which is consistent with the findings of Wan et al. [27]. As shown in Figure 5, when the recombinant strain is cultured with 5% glucose and dextrin as substrates, curdlan yields are 29.38 ± 2.1 g/L and 30.40 ± 1.4 g/L, with gel strengths of 657.8 ± 21.6 and 703.5 ± 34.2 g/cm², respectively. Moreover, the molecular weight of the product from the recombinant strain (3.58×10^6 Da) is higher than that of curdlan (2.69×10^6 Da), representing a 33% increase in molecular weight. When the recombinant strain was cultured with 12% dextrin as the substrate, the curdlan yield was 56.6 ± 1.6 g/L, with a gel strength of 871.2 ± 27.9 g/cm². In contrast, almost no curdlan was produced when 12% glucose was used as the substrate, possibly due to the higher concentration of glucose, triggering the glucose effect and proving detrimental to bacterial growth. When glucose is used as a carbon source, it is typically added separately [37]. Additionally, a high concentration of added glucose may result in the coloration of the synthesized curdlan, necessitating additional steps for decolorization, thereby increasing the complexity of subsequent product processing. Thus, the construction of this recombinant strain is important for the production and processing of curdlan.

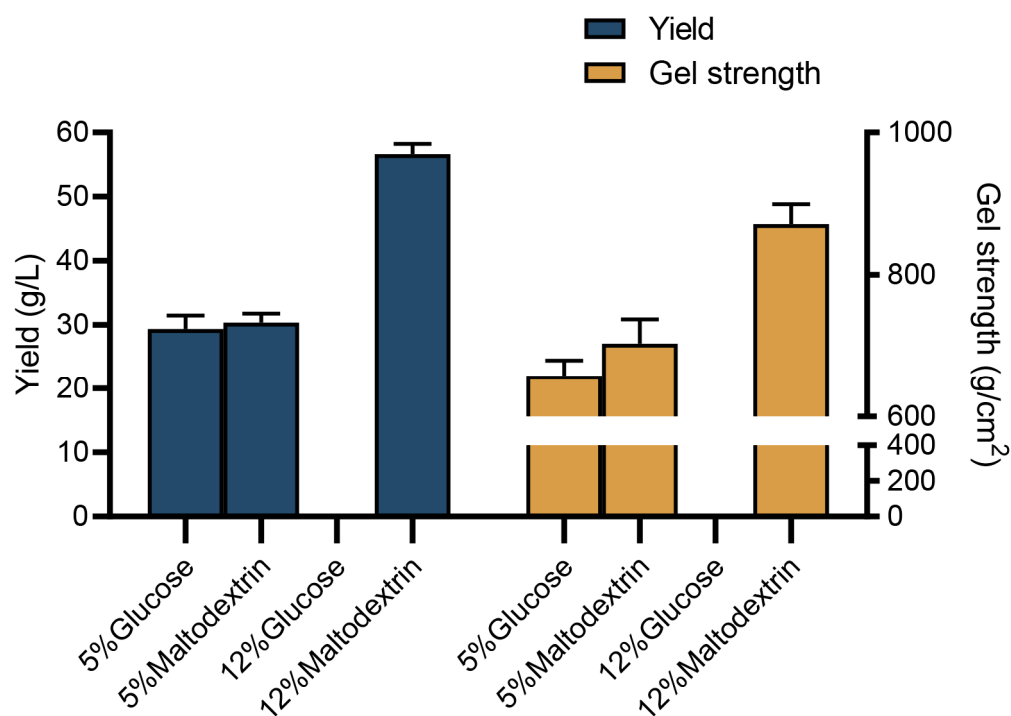


Figure 5. Fermentation characteristics of recombinant strain for curdlan production under glucose and dextrin substrate conditions.

3.4. Batch Fermentation of *sp-AmyAXCC* with Dextrin as Carbon Source

To validate the ability of *sp-AmyAXCC* to utilize dextrin to produce curdlan, batch fermentation was carried out in a 10 L stirred fermenter (Figure 6). As a carbon source, dextrin was added to the fermentation broth at an initial concentration of 120 g/L. However, it was difficult to quantify dextrin during fermentation; thus, the concentration was not recorded. pH is a key factor influencing curdlan synthesis [37]. The optimal initial pH for cell growth is 7.0; whereas the optimal pH for curdlan production is 7.0 or 5.5–6.2. The initial pH of the fermentation broth was set at 7.0 to facilitate bacterial growth. The pH decreased from 7.0 to 5.8 and remained stable throughout the fermentation process, making it suitable for curdlan synthesis. IPTG was added into the culture after 5 h of inoculation to a final concentration of 0.5 mM to induce the expression of α -amylase. The α -amylase activity

increased continuously after induction and reached the maximum value of 1954.9 U/mL at 72 h of fermentation. Curdlan was successfully synthesized from dextrin using exogenous α -amylase. Although the α -amylase activity decreased gradually after 84 h to a final value of 1678.2 U/mL, the titer of curdlan continued to increase and even reached a rather high growth rate during 84–108 h. This may be because the products of dextrin degradation, maltose, and glucose, which can be naturally utilized by *Agrobacterium* sp., accumulate in the fermentation broth and can be rapidly utilized to produce curdlan. At 108 h, the titer of curdlan was 66.7 g/L, with a yield of 0.56 g/g and a productivity of 0.62 g/L/h. Furthermore, the gel strength of the curdlan products was assayed during fermentation. This value increased continuously and reached 972.5 g/cm² after 108 h. Through the specific fermentation results in Table 3, we found that the yield performance of this strain is very impressive in the case of dextrin as substrate. Compared to other substrates, dextrin as a substrate also has the potential to achieve high yields of available curdlan.

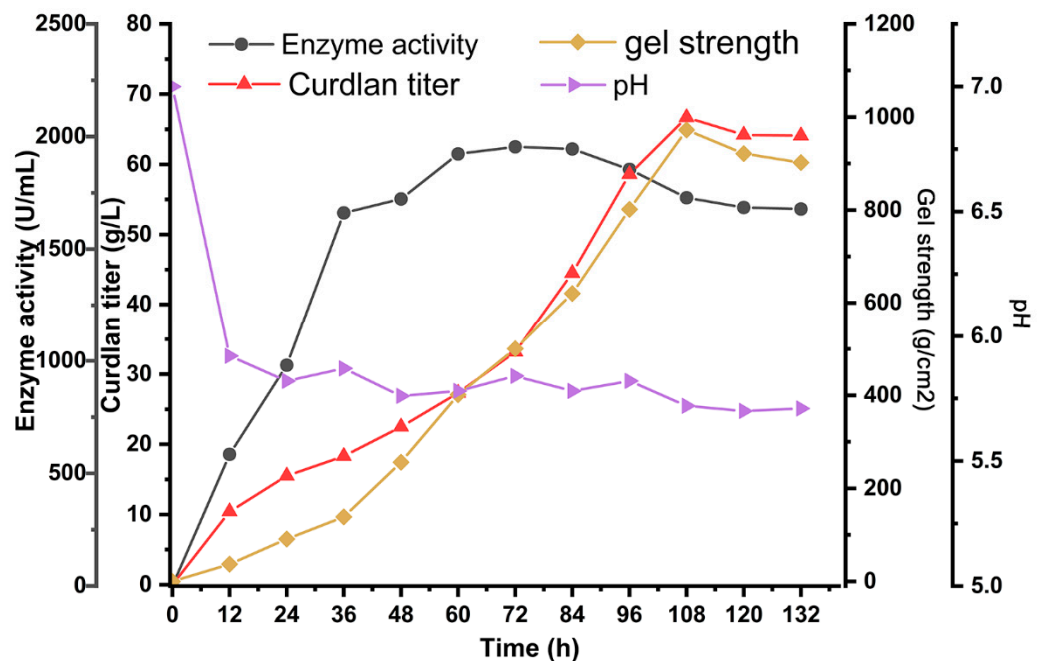


Figure 6. Profile of curdlan fermentation with sp-AmyAXCC using dextrin as carbon source.

Table 3. Curdlan production rates of *Agrobacterium* strain: comparison of substrates.

Strains	Substrate	Substrate(g/L)	Titer (g/L)	Yield (g Curdlan/g Substrate)	Productivity (g/L/h)	Reference
sp-AmyAXCC	Dextrin	120.0	66.7	0.56	0.62	This study
ATCC31749	Sucrose	90.0	38.6	0.43	0.40	[23]
ATCC31749	Sucrose	90.0	48.0	0.79	0.33	[23]
ATCC31749	Maltose	90.0	36.5	0.41	0.38	[23]
ATCC31749	Mannitol	90.0	42.4	0.47	0.44	[23]
ATCC31749	Glucose	80.0	21.9	0.44	0.30	[24]
ATCC31749	Wheat bran	80.0	47.9	0.6	0.33	[24]
ATCC31749	Glucose	50.0	14.4	0.29	0.20	[38]
ATCC31749	Cellobiose	50.0	11.2	0.3	0.15	[28]
ATCC31749 with pHCE-CBP	Cellobiose	50.0	25.9	0.55	0.36	[28]
ATCC31749	Asparagus spear juice	50.0	40.2	0.56	0.24	[39]
ATCC31749	Prairie cordgrass	10.0	9.9	0.01	0.07	[40]
ATCC31749	Cassava starch waste	20.0	21.2	0.40	0.22	[41]
ATCC31749	Glucose	40.0	72.0	0.61	0.75	[19]

3.5. Characterization of Curdlan Product

The characteristics of the product were compared with curdlan, including ATR-FTIR spectrum, X-ray diffraction, gel strength, and molecular weight. As shown in Figure 7, the FTIR spectrum of the samples exhibited characteristic peaks common to curdlan (3323, 2950, 1366, 1156, 887 cm^{-1}), similar to the results of previous studies on curdlan [24]. A broad peak at 3323 cm^{-1} indicates O-H stretching due to hydrogen bonding, and the symmetric $-\text{CH}_2-$ stretching vibration is observed at 2950 cm^{-1} . A characteristic peak representing C=O stretching vibration was observed at 1156 cm^{-1} , and a broad peak at 887 cm^{-1} indicates the linear β -1,3-glucan structure [42]. The X-ray diffraction results showed characteristic diffraction peaks at 19.8° and 29.8° , which closely aligned with those of curdlan in the recombinant strain product. From the above experimental results, it can be proved that the fermentation product of the recombinant strain is consistent with the structure of the available curdlan. When the recombinant strain was cultured with 12% dextrin as substrate, the gel strength of the product was $871.2 \pm 27.9 \text{ g/cm}^2$, which increased by 26.2% ($690.1 \pm 30.7 \text{ g/cm}^2$) compared with that of the curdlan gel. And the molecular weight of the product of the recombinant strain ($3.58 \times 10^6 \text{ Da}$) was higher than that of curdlan ($2.69 \times 10^6 \text{ Da}$) with a 33% increase in molecular weight.

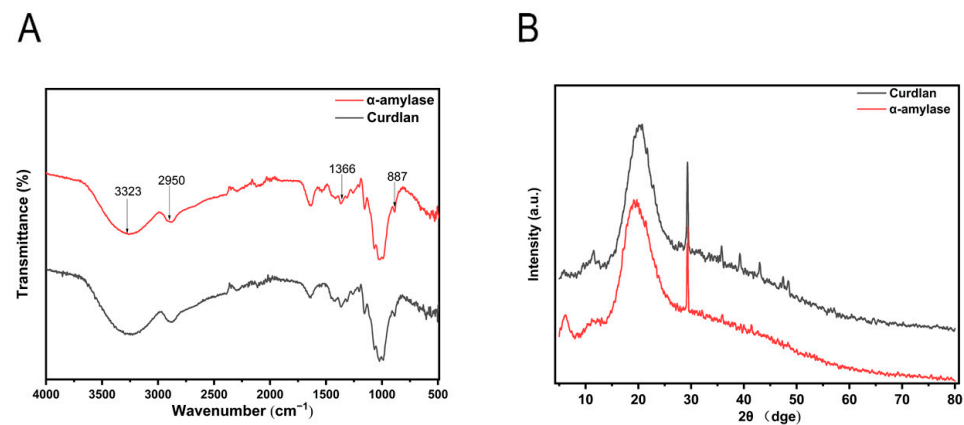


Figure 7. Comparison of the characteristics of curdlan produced by the recombinant strain and ATCC31749. (A) ATR-FTIR spectra of curdlan produced by the recombinant strain and ATCC31749; (B) XRD spectra of curdlan produced by the recombinant strain and ATCC31749.

4. Conclusions

In this study, a recombinant strain, sp-AmyAXCC, with an IPTG-induced heterogeneous α -amylase, was successfully constructed based on strain *A. tumefaciens* ATCC31749. Protein expression of the recombinant strain was analyzed by western blotting. The target protein exhibited an amylase activity of 584.5 U/mL and a specific activity of 5467 U/mg. Compared to the wild-type strain, the recombinant strain demonstrated the ability to utilize dextrin as a fermentation substrate to synthesize curdlan. In the batch fermentation of sp-AmyAXCC with 12% dextrin as a carbon source, the titer of curdlan was 66.7 g/L, with a yield of 0.56 g/g and a productivity of 0.62 g/L/h at 108 h. The gel strength of curdlan reached 972.5 g/cm^2 . Structural characteristics of the curdlan produced by the recombinant strain were similar to those produced by the wild-type strain. This study expands the substrate range of curdlan production to dextrin, providing new scopes for reducing curdlan production costs and enhancing curdlan yield.

Author Contributions: Conceptualization, X.D.; data curation, T.Y. and Y.W.; formal analysis, T.Y., W.W. and H.H.; funding acquisition, X.D.; investigation, T.Y. and Y.W.; methodology, T.Y. and W.W.; project administration, S.Z.; resources, Y.Z. (Yonggang Zhang) and Y.Z. (Yanmin Zhang); supervision, Y.Z. (Yonggang Zhang) and X.D.; validation, Y.Z. (Yanmin Zhang); writing—original draft, T.Y. and Y.W.; writing—review and editing, Y.L. and X.D. All authors have read and agreed to the published version of the manuscript.

Funding: This work was supported by the National Key Research and Development Program of China (2021YFC2103200) and Major innovation projects in science, education, and industry (2022JBZ01-08).

Institutional Review Board Statement: Not applicable.

Informed Consent Statement: Not applicable.

Data Availability Statement: The data that support the findings of this study are available on request from the corresponding author, [X.D.], upon reasonable request.

Acknowledgments: We sincerely thank Tianyi Jiang (Shandong Jianzhu University) for providing crucial guidance in conceptualizing experimental strategies, managing, and coordinating the entire experimental process, as well as offering professional advice on the revision and review of the initial draft of the paper. We express our heartfelt gratitude to Jiang for his assistance, as his contributions have played a crucial role in refining this paper.

Conflicts of Interest: The authors declare no conflicts of interest.

References

- Hundscheil, C.S.; Wagemans, A.M. Rheology of common uncharged exopolysaccharides for food applications. *Curr. Opin. Food Sci.* **2019**, *27*, 1–7. [[CrossRef](#)]
- Gieroba, B.; Sroka-Bartnicka, A.; Kazimierczak, P.; Kalisz, G.; Pieta, I.S.; Nowakowski, R.; Pisarek, M.; Przekora, A. Effect of gelation temperature on the molecular structure and physicochemical properties of the curdolan matrix: Spectroscopic and microscopic analyses. *Int. J. Mol. Sci.* **2020**, *21*, 6154. [[CrossRef](#)] [[PubMed](#)]
- Harada, T. Succinoglucan 10C3: A new acidic polysaccharide of *Alcaligenes faecalis* var. *myxogenes*. *Arch. Biochem. Biophys.* **1965**, *112*, 65–69. [[CrossRef](#)] [[PubMed](#)]
- Verma, D.K.; Niamah, A.K.; Patel, A.R.; Thakur, M.; Sandhu, K.S.; Chávez-González, M.L.; Shah, N.; Aguilar, C.N. Chemistry and microbial sources of curdolan with potential application and safety regulations as prebiotic in food and health. *Food Res. Int.* **2020**, *133*, 109136. [[CrossRef](#)]
- Chen, Y.; Wang, F. Review on the preparation, biological activities and applications of curdolan and its derivatives. *Eur. Polym. J.* **2020**, *141*, 110096. [[CrossRef](#)]
- Zhu, F.; Du, B.; Xu, B. A critical review on production and industrial applications of beta-glucans. *Food Hydrocoll.* **2016**, *52*, 275–288. [[CrossRef](#)]
- Bao, M.; Ehexige, E.; Xu, J.; Ganbold, T.; Han, S.; Baigude, H. Oxidized curdolan activates dendritic cells and enhances antitumor immunity. *Carbohydr. Polym.* **2021**, *264*, 117988. [[CrossRef](#)] [[PubMed](#)]
- Wang, D.; Kim, D.H.; Yoon, J.-J.; Kim, K.H. Production of high-value β -1, 3-glucooligosaccharides by microwave-assisted hydrothermal hydrolysis of curdolan. *Process Biochem.* **2017**, *52*, 233–237. [[CrossRef](#)]
- Yang, X.; Zheng, M.; Hao, S.; Shi, H.; Lin, D.; Chen, X.; Becvarovski, A.; Pan, W.; Zhang, P.; Hu, M. Curdolan prevents the cognitive deficits induced by a high-fat diet in mice via the gut-brain axis. *Front. Neurosci.* **2020**, *14*, 384. [[CrossRef](#)]
- Vessella, G.; Esposito, F.; Traboni, S.; Di Meo, C.; Iadonisi, A.; Schiraldi, C.; Bedini, E. Exploiting diol reactivity for the access to unprecedented low molecular weight curdolan sulfate polysaccharides. *Carbohydr. Polym.* **2021**, *269*, 118324. [[CrossRef](#)]
- Sato, F.; Nakamura, Y.; Katsuki, A.; Khadka, S.; Ahmad, I.; Omura, S.; Martinez, N.E.; Tsunoda, I. Curdolan, a microbial β -glucan, has contrasting effects on autoimmune and viral models of multiple sclerosis. *Front. Cell. Infect. Microbiol.* **2022**, *12*, 16. [[CrossRef](#)] [[PubMed](#)]
- Cai, Z.; Zhang, H. Recent progress on curdolan provided by functionalization strategies. *Food Hydrocoll.* **2017**, *68*, 128–135. [[CrossRef](#)]
- Nurzynska, A.; Klimek, K.; Swierzycka, I.; Palka, K.; Ginalska, G. Porous curdolan-based hydrogels modified with copper ions as potential dressings for prevention and management of bacterial wound infection—An in vitro assessment. *Polymers* **2020**, *12*, 1893. [[CrossRef](#)] [[PubMed](#)]
- Suflet, D.M.; Popescu, I.; Prisacaru, A.I.; Pelin, I.M. Synthesis and characterization of curdolan-phosphorylated curdolan based hydrogels for drug release. *Int. J. Polym. Mater.* **2021**, *70*, 870–879. [[CrossRef](#)]
- Han, J.; Wang, X.; Liu, L.; Li, D.; Suyaola, S.; Wang, T.; Baigude, H. “Click” chemistry mediated construction of cationic curdolan nanocarriers for efficient gene delivery. *Carbohydr. Polym.* **2017**, *163*, 191–198. [[CrossRef](#)] [[PubMed](#)]
- Yan, J.-K.; Pei, J.-J.; Ma, H.-L.; Wang, Z.-B. Effects of ultrasound on molecular properties, structure, chain conformation and degradation kinetics of carboxylic curdolan. *Carbohydr. Polym.* **2015**, *121*, 64–70. [[CrossRef](#)] [[PubMed](#)]
- Wan, J.; Wang, Y.; Jiang, D.; Gao, H.; Yang, G.; Yang, X. Effects of carbon sources on production and properties of curdolan using *Agrobacterium* sp. DH-2. *Prep. Biochem. Biotech.* **2020**, *50*, 857–864. [[CrossRef](#)] [[PubMed](#)]
- Ben Salah, R.; Jaouadi, B.; Bouaziz, A.; Chaari, K.; Blecker, C.; Derrouane, C.; Attia, H.; Besbes, S. Fermentation of date palm juice by curdolan gum production from *Rhizobium radiobacter* ATCC 6466TM: Purification, rheological and physico-chemical characterization. *LWT-Food Sci. Technol.* **2011**, *44*, 1026–1034. [[CrossRef](#)]

19. Mohsin, A.; Sun, J.; Khan, I.M.; Hang, H.; Tariq, M.; Tian, X.; Ahmed, W.; Niazi, S.; Zhuang, Y.; Chu, J. Sustainable biosynthesis of curdlan from orange waste by using *Alcaligenes faecalis*: A systematically modeled approach. *Carbohydr. Polym.* **2019**, *205*, 626–635. [[CrossRef](#)]
20. Prakash, S.; Rajeswari, K.; Divya, P.; Ferlin, M.; Rajeshwari, C.T.; Vanavil, B. Optimization and production of curdlan gum using *Bacillus cereus* PR3 isolated from rhizosphere of leguminous plant. *Prep. Biochem. Biotech.* **2018**, *48*, 408–418. [[CrossRef](#)]
21. Yuan, M.; Fu, G.; Sun, Y.; Zhang, D. Biosynthesis and applications of curdlan. *Carbohydr. Polym.* **2021**, *273*, 118597. [[CrossRef](#)] [[PubMed](#)]
22. Yu, X.; Zhang, C.; Yang, L.; Zhao, L.; Lin, C.; Liu, Z.; Mao, Z. CrdR function in a curdlan-producing *Agrobacterium* sp. ATCC31749 strain. *BMC Microbiol.* **2015**, *15*, 25. [[CrossRef](#)] [[PubMed](#)]
23. Gao, H.; Xie, F.; Zhang, W.; Tian, J.; Zou, C.; Jia, C.; Jin, M.; Huang, J.; Chang, Z.; Yang, X. Characterization and improvement of curdlan produced by a high-yield mutant of *Agrobacterium* sp. ATCC 31749 based on whole-genome analysis. *Carbohydr. Polym.* **2020**, *245*, 116486. [[CrossRef](#)]
24. Liang, Y.; Zhu, L.; Ding, H.; Gao, M.; Zheng, Z.; Wu, J.; Zhan, X. Enhanced production of curdlan by coupled fermentation system of *Agrobacterium* sp. ATCC 31749 and *Trichoderma harzianum* GIM 3.442. *Carbohydr. Polym.* **2017**, *157*, 1687–1694. [[CrossRef](#)]
25. Liang, Y.; Zhu, L.; Gao, M.; Zheng, Z.; Wu, J.; Zhan, X. Influence of Tween-80 on the production and structure of water-insoluble curdlan from *Agrobacterium* sp. *Int. J. Biol. Macromol.* **2018**, *106*, 611–619. [[CrossRef](#)] [[PubMed](#)]
26. Yang, M.; Zhu, Y.; Li, Y.; Bao, J.; Fan, X.; Qu, Y.; Wang, Y.; Hu, Z.; Li, Q. Production and optimization of curdlan produced by *Pseudomonas* sp. QL212. *Int. J. Biol. Macromol.* **2016**, *89*, 25–34. [[CrossRef](#)] [[PubMed](#)]
27. Wan, J.; Shao, Z.; Jiang, D.; Gao, H.; Yang, X. Curdlan production from cassava starch hydrolysates by *Agrobacterium* sp. DH-2. *Bioproc. Biosyst. Eng.* **2022**, *45*, 969–979. [[CrossRef](#)] [[PubMed](#)]
28. Shin, H.-D.; Liu, L.; Kim, M.-K.; Park, Y.-I.; Chen, R. Metabolic engineering of *Agrobacterium* sp. ATCC31749 for curdlan production from cellobiose. *J. Ind. Microbiol. Biot.* **2016**, *43*, 1323–1331. [[CrossRef](#)]
29. Gao, M.; Liu, Z.; Zhao, Z.; Wang, Z.; Hu, X.; Jiang, Y.; Yan, J.; Li, Z.; Zheng, Z.; Zhan, X. Exopolysaccharide synthesis repressor genes (exoR and exoX) related to curdlan biosynthesis by *Agrobacterium* sp. *Int. J. Biol. Macromol.* **2022**, *205*, 193–202. [[CrossRef](#)]
30. Kerdsup, P.; Tantratian, S.; Sanguandeeikul, R.; Imjongjirak, C. Xanthan production by mutant strain of *Xanthomonas campestris* TISTR 840 in raw cassava starch medium. *Food Bioprocess Tech.* **2011**, *4*, 1459–1462. [[CrossRef](#)]
31. Xiao, Z.; Storms, R.; Tsang, A. A quantitative starch: Iodine method for measuring alpha-amylase and glucoamylase activities. *Anal. Biochem.* **2006**, *351*, 146–148. [[CrossRef](#)] [[PubMed](#)]
32. Gao, H.; Zhang, W.; Zhang, J.; Huang, Y.; Zhang, J.; Tian, J.; Niu, Y.; Zou, C.; Jia, C.; Chang, Z. Methionine biosynthesis pathway genes affect curdlan biosynthesis of *Agrobacterium* sp. CGMCC 11546 via energy regeneration. *Int. J. Biol. Macromol.* **2021**, *185*, 821–831. [[CrossRef](#)]
33. Szwengiel, A.; Wiesner, M. Effect of metal ions on levan synthesis efficiency and its parameters by levansucrase from *Bacillus subtilis*. *Int. J. Biol. Macromol.* **2019**, *128*, 237–243. [[CrossRef](#)] [[PubMed](#)]
34. Yu, L.; Wu, J.; Liu, J.; Zhan, X.; Zheng, Z.; Lin, C.C. Enhanced curdlan production in *Agrobacterium* sp. ATCC 31749 by addition of low-polyphosphates. *Biotechnol. Bioprocess Eng.* **2011**, *16*, 34–41. [[CrossRef](#)]
35. Sèbe, G.; Ham-Pichavant, F.; Pecastaings, G. Dispersibility and emulsion-stabilizing effect of cellulose nanowhiskers esterified by vinyl acetate and vinyl cinnamate. *Biomacromolecules* **2013**, *14*, 2937–2944. [[CrossRef](#)]
36. Abe, J.-i.; Onitsuka, N.; Nakano, T.; Shibata, Y.; Hizukuri, S.; Entani, E. Purification and characterization of periplasmic alpha-amylase from *Xanthomonas campestris* K-11151. *J. Bacteriol.* **1994**, *176*, 3584–3588. [[CrossRef](#)] [[PubMed](#)]
37. Yang, H.; Li, W.; Chen, S.; Guo, X.; Huang, F.; Zhu, P. Optimization and modeling of curdlan production under multi-physiological-parameters process control by *Agrobacterium radiobacter* mutant A-15 at high initial glucose. *Biotechnol. Bioprocess Eng.* **2021**, *26*, 1012–1022. [[CrossRef](#)]
38. Liu, Z.; Xu, Y.; Wang, Z.; Zhu, L.; Li, Z.; Jiang, Y.; Zhan, X.; Gao, M. Promoting substrates uptake and curdlan synthesis of *Agrobacterium* sp. by attenuating the exopolysaccharide encapsulation. *Carbohydr. Polym.* **2023**, *315*, 120941. [[CrossRef](#)]
39. Anane, R.F.; Sun, H.; Zhao, L.; Wang, L.; Lin, C.; Mao, Z. Improved curdlan production with discarded bottom parts of Asparagus spear. *Microb. Cell Factories* **2017**, *16*, 1–8. [[CrossRef](#)] [[PubMed](#)]
40. West, T.P. Effect of nitrogen source concentration on curdlan production by *Agrobacterium* sp. ATCC 31749 grown on prairie cordgrass hydrolysates. *Prep. Biochem. Biotech.* **2016**, *46*, 85–90. [[CrossRef](#)]
41. Wu, S.; Lu, M.; Fang, Y.; Wu, L.; Xu, Y.; Wang, S. Production of curdlan grown on cassava starch waste hydrolysates. *J. Polym. Environ.* **2018**, *26*, 33–38. [[CrossRef](#)]
42. Binder, D.; Frohwitter, J.; Mahr, R.; Bier, C.; Grünberger, A.; Loeschcke, A.; Peters-Wendisch, P.; Kohlheyer, D.; Pietruszka, J.; Frunzke, J. Light-controlled cell factories: Employing photocaged isopropyl-β-d-thiogalactopyranoside for light-mediated optimization of lac promoter-based gene expression and (+)-valencene biosynthesis in *Corynebacterium glutamicum*. *Appl. Environ. Microb.* **2016**, *82*, 6141–6149. [[CrossRef](#)] [[PubMed](#)]

Disclaimer/Publisher’s Note: The statements, opinions and data contained in all publications are solely those of the individual author(s) and contributor(s) and not of MDPI and/or the editor(s). MDPI and/or the editor(s) disclaim responsibility for any injury to people or property resulting from any ideas, methods, instructions or products referred to in the content.